High-Resolution Crystal Structures of Drosophila melanogaster Angiotensin-Converting Enzyme in Complex with Novel Inhibitors and Antihypertensive Drugs

ARTICLE *in* JOURNAL OF MOLECULAR BIOLOGY · JULY 2010

Impact Factor: 4.33 · DOI: 10.1016/j.jmb.2010.05.024 · Source: PubMed

doi:10.1016/j.jmb.2010.05.024 J. Mol. Biol. (2010) 400, 502–517

JMB

Available online at www.sciencedirect.com

ScienceDirect

ELSEVIER

High-Resolution Crystal Structures of *Drosophila melanogaster* Angiotensin-Converting Enzyme in Complex with Novel Inhibitors and Antihypertensive Drugs

Mohd Akif[1], Dimitris Georgiadis[2], Aman Mahajan[3], Vincent Dive[4], Edward D. Sturrock[3], R. Elwyn Isaac[5] and K. Ravi Acharya[1]*

[1]*Department of Biology and Biochemistry, University of Bath, Claverton Down, Building 4 South, Bath BA2 7AY, UK*

[2]*Department of Chemistry, Laboratory of Organic Chemistry, University of Athens, Panepistimiopolis Zografou, 15771 Athens, Greece*

[3]*Division of Medical Biochemistry and Institute of Infectious Disease and Molecular Medicine, University of Cape Town, Cape Town, Observatory 7925, South Africa*

[4]*CEA, iBiTecS, Service d'Ingénierie Moléculaire des Protéines (SIMOPRO), F-91191 Gif sur Yvette, France*

[5]*Institute of Integrative and Comparative Biology, Faculty of Biological Sciences, Clarendon Way, University of Leeds, Leeds LS2 9JT, UK*

Received 8 April 2010; received in revised form 10 May 2010; accepted 11 May 2010
Available online 19 May 2010

Edited by I. Wilson

Angiotensin I-converting enzyme (ACE), one of the central components of the renin–angiotensin system, is a key therapeutic target for the treatment of hypertension and cardiovascular disorders. Human somatic ACE (sACE) has two homologous domains (N and C). The N- and C-domain catalytic sites have different activities toward various substrates. Moreover, some of the undesirable side effects of the currently available and widely used ACE inhibitors may arise from their targeting both domains leading to defects in other pathways. In addition, structural studies have shown that although both these domains have much in common at the inhibitor binding site, there are significant differences and these are greater at the peptide binding sites than regions distal to the active site. As a model system, we have used an ACE homologue from *Drosophila melanogaster* (AnCE, a single domain protein with ACE activity) to study ACE inhibitor binding. In an extensive study, we present high-resolution structures for native AnCE and in complex with six known antihypertensive drugs, a novel C-domain sACE specific inhibitor, lisW-S, and two sACE domain-specific phosphinic peptidyl inhibitors, RXPA380 and RXP407 (i.e., nine structures). These structures show detailed binding features of the inhibitors and highlight subtle changes in the orientation of side chains at different binding pockets in the active site in comparison with the active site of N- and C-domains of sACE. This study provides information about the structure–activity relationships that could be utilized for designing new inhibitors with improved domain selectivity for sACE.

Keywords: angiotensin-converting enzyme; zinc metallopeptidase; hypertension; X-ray crystallography; inhibitor binding

*Corresponding author. E-mail address: K.R.Acharya@bath.ac.uk.

Abbreviations used: ACE, angiotensin-converting enzyme; RAAS, renin–angiotensin–aldosterone system; tACE, human testis angiotensin I-converting enzyme; sACE, somatic angiotensin I-converting enzyme; lisW-S, lisinopril–tryptophan *S*-enantiomer; RXPA380, (2*S*)-2-[({2-[(1*R*)-1-[((benzyloxy)carbonyl)amino]-2-(phenylethyl)(hydroxyl)-phosphinyl]cyclopentyl}carbonyl)amino]-3-(1*H*-indo-3-yl)-propionic acid (Cbz-PheΨ[P(O)(OH)CH]Pro-Trp-OH); RXP407, Ac-Asp-$_{(L)}$Phe(PO_2CH_2)$_{(L)}$Ala-Ala-NH_2.

Introduction

Angiotensin I-converting enzyme (ACE, EC 3.4.15.1) is a zinc metallopeptidase that plays a critical role in blood pressure regulation by catalyzing the proteolysis of angiotensin I to the vasopressor angiotensin II.[1–4] ACE is a critical component of the renin–angiotensin–aldosterone system (RAAS), which controls blood pressure and strongly influences the function of the heart and the kidneys, as well as contraction of blood vessels.[5] For these reasons, drugs that target the RAAS—including ACE inhibitors, angiotensin II receptor blockers, renin inhibitors and aldosterone antagonists—are among the most important therapeutic agents available today for the treatment of hypertension, heart failure and renal insufficiency.

There are two isoforms of human ACE; in somatic tissues, it exists as a glycoprotein composed of a mature single large polypeptide chain of 1277 amino acids [somatic ACE (sACE)] (the extracellular domain of the full-length membrane protein) with two domains (N and C), each containing an active center.[6] Testis ACE (tACE) is identical to the C-terminal half of sACE, except for a unique 36-residue sequence constituting its amino terminus.[7] Both domains are heavily glycosylated—a feature that has hampered the three-dimensional structure determination of the protein for a long time. Despite sharing ~60% sequence identity with the C-domain, the N-domain of sACE has its own distinctive physicochemical and functional properties. It is thermally more stable than the C-domain,[8] more resistant to proteolysis under denaturing conditions[9] and is less dependent on chloride activation as compared with the C-domain.[10,11] Substrates, such as the hemoregulatory peptide AcSDKP (acetyl-Ser-Asp-Lys-Pro),[12] angiotensin 1–7,[13] and the enkephalin precursor Met^5-Enk-Arg^6-Phe^7,[14] are specific for the N-domain hydrolysis, whereas the physiological substrates bradykinin and angiotensin I are hydrolysed with similar catalytic efficiency as the C-domain.

To date, crystal structures of tACE in complex with a few potent inhibitors[15–19] and N-domain of sACE in the presence of lisinopril, an antihypertensive drug,[20] are known. They have provided details of the substrate-binding pocket as well as Cl^--binding residues and their potential interactions and selectivity. These studies have clearly established that the two domains of sACE have differences mainly attributed to subtle variation of residues at the binding pocket of the protein and suggest additional clues for structure-based drug design of potent inhibitors.

In 1977, Cushman *et al.* described the synthesis of a series of potent inhibitors of sACE designed on the basis of an assumed mechanistic homology with carboxypeptidase A.[21] This ushered in a generation of drugs for the management of hypertension, many of which are still used today. These inhibitors were developed without the benefit of any detailed chemical, kinetic or structural information on ACE. Despite the success of these ACE inhibitors, many patients (~25%) have difficulty with long-term treatment with current-generation ACE inhibitors because of side effects, most commonly a persistent dry cough and in some cases a more serious adverse effect known as angioedema.[22] These adverse effects are likely related to the fact that treatment with current-generation ACE inhibitors not only inhibits the production of angiotensin II, but also affects the levels of other active peptides, with not well understood consequences. A further problem is that in some patients, chronic therapy with current-generation ACE inhibitors results in reduced efficacy over time, sometimes termed as "ACE inhibitor escape phenomenon," indicating that the potency of current-generation ACE inhibitors can be improved by, for instance, the design of irreversible ACE inhibitors that block the active site. The structures of tACE and N-domain of sACE provide a platform for the design of domain-selective inhibitors (i.e., next generation of ACE inhibitors).

It is now clear that next-generation ACE inhibitors are required that selectively and potently inhibit either the N- or the C-domain. Based on current knowledge, inhibitors of the C-domain are likely to have effects on cardiovascular function similar to those of current-generation ACE inhibitors, but without undesired side effects largely due to decreased bradykinin and substance P levels.

Rational structure-based design of potent and selective peptide-based domain-specific ACE inhibitors using sACE protein has not been an easy task due to the presence of several glycosylation sites in both domains. Meanwhile, we have used a homologue of ACE from *Drosophila melanogaster*, AnCE, a single domain protein with ACE-like activity,[23] to obtain proof-of-principle structural data for rational design of new ACE inhibitors. It has been established that AnCE resembles the C-domain of sACE[24] including the shared functional conserved active site.[25,26] Hence, we have chosen AnCE as a model system to study binding of currently known (and marketed) ACE inhibitors and newly identified potent domain-specific inhibitors of sACE. The structure of native AnCE protein (at 2.6 Å resolution) and in the presence of captopril and lisinopril (at 2.4 Å resolution) (form I in monoclinic space group $P2_1$) have been determined previously.[27]

In this comprehensive study, we present a new and high-resolution structure of AnCE (form II in trigonal *R*3 space group) along with nine structures of AnCE in complex with known antihypertensive drugs—captopril, enalaprilat, lisinopril, ramiprilat, trandolaprilat, perindoprilat—as well as a novel derivative of lisinopril, lisW-S (lisinopril–tryptophan *S*-enantiomer) and with domain-selective phosphinic peptidyl inhibitors, RXPA380 [(2*S*)-2-[({2-[(1*R*)-1-[((benzyloxy)carbonyl)amino]-2-(phenylethyl)(hydroxyl)-phosphinyl]cyclopentyl}carbonyl)amino]-3-(1*H*-indo-3-yl)-propionic acid (Cbz-PheΨ[P(O)(OH)CH]Pro-Trp-OH)] (C-domain selective) and RXP407 [Ac-Asp-$_{(L)}$Phe(PO_2CH_2)$_{(L)}$Ala-Ala-NH_2] (N-domain selective) in the range of

1.85–2.0 Å resolution (Fig. 1 and Table 1). These structures provide a detailed framework of key residues involved in inhibitor recognition.

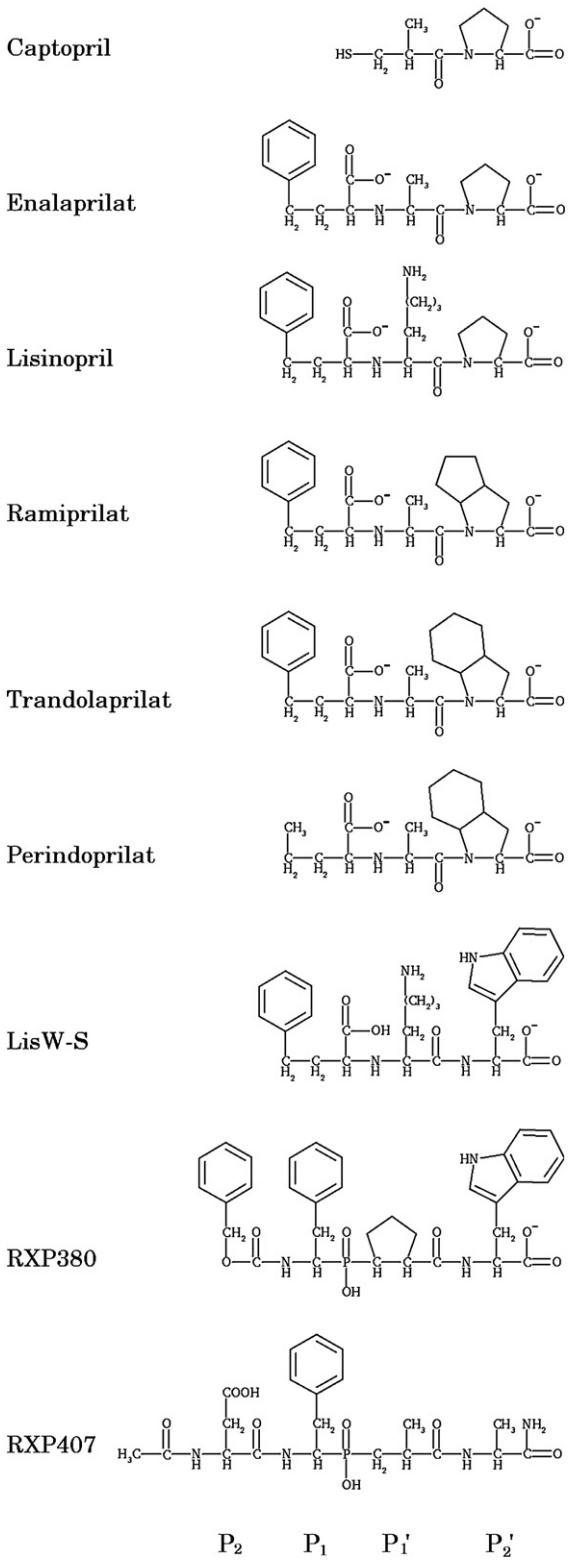

Fig. 1. Chemical structure of ACE inhibitors showing residue positions (P_2, P_1, P_1' and P_2') labeled relative to the zinc-binding group.

Results and Discussion

Overall structure of native AnCE and inhibitor complexes

The final native structure of AnCE contains amino acid residues from 20 to 614 (residues 17–614 in all structures of complexes), which are arranged predominantly in a helical conformation containing 21 α-helices, nine 3_{10} short helices and two antiparallel β-strands, similar to already reported AnCE (form I structure),[27] tACE[15] and N-domain of sACE structures.[20] The structure was modelled with a catalytic Zn^{2+} ion at the conserved active site deep inside the molecule and a citrate ion (from the crystallization medium) (Fig. 2a). In the present high-resolution native AnCE (form II) structure, additional features include oligosaccharide chains at the N-glycosylation sites (Fig. 2a; see below). In addition, a total of 695 water molecules were modelled by the program WATERPICK in COOT,[28] and the location of these water molecules was confirmed by examining the difference electron density maps visually on the graphics. Similar numbers of water molecules were identified in the inhibitor-bound structures of complexes. In all structures, 25–30 water molecules were found at the N-terminal opening of the active-site cavity. In addition, one to three Hepes molecules (from the crystallization medium) were found trapped at this site. In the native and captopril complex, only patchy density was observed at these sites and hence could not be modelled with Hepes molecules. Unlike tACE and N-domain structures, no chloride ion binding was observed in the AnCE structure.

The AnCE molecule contains three N-glycosylation sites,[24] and Fourier difference electron density was observed at all three sites in the native (and bound) structure(s). One long chain of sugars containing two *N*-acetyl glucosamine, two β-D-mannose and two α-D-mannose were modelled attaching to Asn196. Disordered electron density was observed at other two N-glycosylation sites, Asn53 and Asn311, and only one *N*-acetyl glucosamine moiety could be modelled at each of these sites (Fig. 2a). The long arm of the carbohydrate chain attached to Asn196 appears to participate in weak ionic interaction with Gln84 of helix 2 at the amino-terminal part of the protein. This interaction could contribute to the stability of the protein, as it has been shown previously that the deglycosylated form of AnCE, although active, seemed less stable.[24] The N-glycosylation site at Asn53 in AnCE is conserved in tACE (Fig. 2a). In tACE, N-glycosylation at this site has been shown to be crucial for processing and activity of the tACE.[29]

AnCE was also crystallized in the presence of known antihypertensive drugs and newly designed inhibitors such as RXPA380, RXP407 and lisW-S (Fig. 1), for which clear Fourier difference electron density was observed upon refinement (Figs. 3 and 4). In all nine structures of complexes presented

Table 1. Diffraction data and refinement statistics for AnCE–inhibitor complexes

	AnCE	Captopril	Enalaprilat	Lisinopril	Ramiprilat
Resolution range (Å)	50.0–1.90	50.0–1.98	50.0–1.98	50.0–1.98	50.0–2.11
Space group (1 mol/a.u.)	*R*3	*R*3	*R*3	*R*3	*R*3
Unit cell parameters (Å and deg)	$a=b=173.09$, $c=101.56$ $\alpha=\beta=90.0$, $\gamma=120.0$	$a=b=173.29$, $c=101.27$ $\alpha=\beta=90.0$, $\gamma=120.0$	$a=b=172.83$, $c=101.87$ $\alpha=\beta=90.0$, $\gamma=120.0$	$a=b=172.80$, $c=101.51$ $\alpha=\beta=90.0$, $\gamma=120.0$	$a=b=173.17$, $c=103.60$ $\alpha=\beta=90.0$, $\gamma=120.0$
No. of total/unique reflections	800,079/89,453	517,126/78,537	384,819/80,053	351,287/79,396	698,341/66,944
Completeness (%)	95.0 (89.0)	96.0 (88.1)	98.2 (93.5)	93.6 (87.6)	94.5 (80.0)
R_{sym} (%)[a]	7.1 (20.7)	6.8 (16.1)	8.5 (29.5)	6.9 (30.2)	14.6 (45.4)
$I/\sigma(I)$ (%)	14.7 (6.4)	13.0 (6.1)	10.0 (3.2)	12.1 (3.1)	8.2 (2.0)
Refinement					
R_{cryst} (%)[b]	19.4	19.5	18.8	19.3	19.1
R_{free} (%)[c]	22.0	21.6	21.4	20.9	21.8
No. of reflections used	83371	72218	74656	70559	59967
No. of water molecules	695	576	670	621	522
Average temperature factor (Å^2)					
Protein atoms	33.6	29.9	26.7	28.5	21.3
Protein main chain	33.2	29.5	26.2	28.1	20.8
Protein side chain	33.9	30.3	27.1	28.9	21.3
Inhibitor atoms	51.6	30.4	24.7	25.7	25.6
Glycosylated sugars	43.7	46.9	41.9	48.7	35.5
Solvent atoms	33.5	30.0	34.0	36.7	29.7
Zn^{2+} ion	33.6	26.1	20.7	21.5	14.2
RMS deviation from ideal values					
Bond length (Å)	0.007	0.007	0.006	0.006	0.006
Bond angles (deg)	0.98	0.98	0.99	0.98	1.00
Ramachandran plot statistics					
% Residues in favoured region	98.6	98.6	98.9	98.9	98.6
PDB code	2X8Y	2X8Z	2X90	2X91	2X92

	Trandolaprilat	Perindoprilat	lisW-S	RXPA380	RXP407
Resolution limits(Å)	50–1.98	50.0–1.88	50.0–1.96	50.0–1.85	50.0–1.85
Space group (1 mol/a.u.)	*R*3	*R*3	*R*3	*R*3	*R*3
Unit cell parameters (Å and deg)	$a=b=172.86$, $c=103.25$ $\alpha=\beta=90.0$, $\gamma=120.0$	$a=b=173.13$, $c=102.28$ $\alpha=\beta=90.0$, $\gamma=120.0$	$a=b=172.63$, $c=102.41$ $\alpha=\beta=90.0$, $\gamma=120.0$	$a=b=173.07$, $c=101.58$ $\alpha=\beta=90.0$, $\gamma=120.0$	$a=b=173.08$, $c=101.90$ $\alpha=\beta=90.0$, $\gamma=120.0$
No. of total/unique reflections	344,648/80,566	436,072/92,711	391,091/81,744	755,742/96,897	483,141/96,735
Completeness (%)	96.9 (87.9)	96.7 (81.0)	87.2 (87.5)	91.0 (66.6)	93.4 (79.9)
R_{sym} (%)[a]	8.3 (25.6)	10.5 (44.2)	8.0 (41.8)	9.0 (23.5)	7.5 (39.8)
I/σ(I) (%)	9.6 (3.7)	7.7 (1.4)	11.3 (3.4)	10.1 (3.7)	10.9 (2.1)
Refinement					
R_{cryst} (%)[b]	19.0	19.4	19.5	19.5	17.3
R_{free} (%)[c]	20.6	21.2	21.7	21.4	20
No. of reflections used	74,104	85,044	67,717	83,805	85,810
No. of water molecules	770	656	766	724	795
Average temperature factor (Å^2)					
Protein atoms	24.4	28.1	26.8	27.9	26.7
Protein main chain	23.9	27.7	26.5	27.6	25.3
Protein side chain	24.7	28.4	27.2	28.2	28.1
Inhibitor atoms	24.0	33.5	32.1	30.6	25.2
Glycosylated sugars	42.0	43.9	44.4	45.4	44.3
Solvent atoms	34.2	37.3	36.8	38.8	37.5
Zn^{2+} ion	19.4	23.2	21.0	22.0	22.5
r.m.s.d. from ideal values					
Bond length (Å)	0.007	0.006	0.006	0.006	0.006
Bond angles (deg)	1.00	0.98	0.99	1.31	0.98
Ramachandran plot statistics					
% Residues in favoured region	98.9	98.9	98.9	98.8	98.5
PDB code	2X93	2X94	2X95	2X96	2X97

Values in parentheses are for the last-resolution shell. a.u., asymmetric unit.

[a] $R_{merge}=\sigma_h\sigma_i[\,|I_i(h)-\langle I(h)\rangle|\,/\sigma_h\sigma_i I_i(h)]$, where I_i is the ith measurement and $\langle I(h)\rangle$ is the weighted mean of all the measurements of $I(h)$.

[b] $R_{cryst}=\sigma_h|F_o-F_c|/\sigma_h F_o$, where F_o and F_c are the observed and calculated structure factor amplitudes of reflection h, respectively.

[c] R_{free} is equal to R_{cryst} for a randomly selected 5% subset of reflections not used in the refinement.

here, the inhibitor molecule is buried deep inside the active-site pocket making direct interaction with the catalytic zinc ion, and no detectable structural change was observed. Similar numbers of water molecules were also identified in the inhibitor-bound structures of complexes at high resolution (1.85–2.1 Å) making the comparison of inhibitor binding features more uniform.

The overall structure of AnCE (form II) is in a conformation similar to that of the previously reported AnCE structure (form I) with an overall r.m.s.d. (all atoms) of 0.52 Å. However, compared to AnCE form I structure, form II is at a higher resolution and contains a large number of well-ordered water molecules surrounding the molecule including the active site (a total of 695 water molecules in form II structure compared with 2 water molecules in form I structure). In addition, residues Gly51, Thr346, Ala547 and Thr607 in form II structure (present study) follow AnCE amino acid sequence and are clearly visible in the electron density map (modelled as Arg51, Ile346, Arg547 and Ile607, respectively, in the form I structure).[27]

Comparison with N- and C-domains of sACE

AnCE shares ~60% sequence similarity with each of the two domains of sACE, and hence has the same overall topology with an r.m.s.d. of 1.19 Å (for 571 C^{α} atoms from the N-domain of sACE) and 1.09 Å (for 556 C^{α} atoms of the C-domain of sACE or tACE), respectively. The active site and the Zn^{2+} ion binding motif are highly conserved among the three structures. However, there are some notable differences at the substrate binding sites S_2, S_1, S_1' and S_2' (Table 2; based on general nomenclature as defined by Schechter and Berger).[30] For example, Phe363 and Thr364 in AnCE at the S_2' subsite are replaced with Val379 and Val380 in the C-domain, while the N-domain has Ser357 and Thr358 at equivalent positions (Fig. 2b). The S_2 subsite of AnCE has residues such as Thr387 and Phe375 that are replaced by Glu403 and Phe391 in the C-domain; the equivalent residues are replaced with Arg381 and Tyr369 in the N-domain structure. Interestingly, the residues present in these subsites of AnCE are not exactly identical with any one of the domains, but does show similarity between both N- and C-domains. This might explain the efficient binding of both domain-selective phosphinic inhibitors to AnCE (see below). However, the catalytic properties, k_{cat}/K_m of AcSDKP hydrolysis and optimal chloride ion concentration, have demonstrated the functional resemblance of AnCE with the C-domain of sACE.[24]

Binding of antihypertensive drugs

Captopril

Captopril is the smallest orally active tight binding peptide analogue inhibitor of both domains of ACE. It has two residues at the P_1' and P_2' position relative to the scissile bond and a free sulfhydryl as a zinc-coordinating group (Fig. 3a). In the AnCE–captopril structure, the thiol-coordinating group of the inhibitor makes a direct interaction with the catalytic Zn^{2+} ion (distance, 2.15 Å) (Fig. 3a). The orientation of the thiol group is quite different from the reported structures of the tACE[16] and AnCE (form I) in complex with captopril[27] and results in the loss of direct interaction with Glu368 (Glu384 in tACE-captopril complex). Additionally, the captopril molecule is held by 8 H-bonds (Table 3), including three with water molecules that are conserved in the tACE–captopril structure.[16] The central carbonyl oxygen positioned between the thiol and the terminal proline moiety of captopril is anchored by two strong H-bonds with His337 and His497. One of the oxygen atoms from the proline moiety's carboxylate group is held by interactions with side chains of residues, Gln265, Lys495 and Tyr504, at the S_2' subsite (Table 3). Interestingly, the second oxygen of the proline moiety's carboxylate group in the present AnCE–captopril complex is held indirectly by water-molecule-mediated interactions with Asn261 and Glu150. Furthermore, a network of water molecules makes indirect interactions between the carboxylate oxygen and with Arg356, Asp360 and Gln361 in the S_1' and S_2' subsites.

Enalaprilat

Enalapril is a prodrug that is the ethyl ester of enalaprilat. Even though we used enalapril in co-crystallization with AnCE, the final structure contains the activated form (enalaprilat) due to hydrolysis of the prodrug in the crystallization medium. The binding of enalaprilat in AnCE is more extensive than that of captopril due to the extension of the phenyl moiety at the P_1 position. Unlike the sulfhydryl group of captopril, the carboxylate group of enalaprilat makes tight coordination with the Zn^{2+} ion at the active site of the protein (distances, 2.00 and 2.57 Å). In addition, enalaprilat is anchored to the protein by 14 H-bonds including 5 H-bonds that are mediated by water molecules (Fig. 3b and Table 3), and its orientation is similar to that of the tACE–enalaprilat structure.[16] The Zn^{2+} ion coordination in enalaprilat probably has positioned the carbonyl group slightly differently from that in the captopril complex and results in the loss of a key H-bond interaction with His497. Similar interaction has been reported in the tACE–enalaprilat complex where His513 appears to be positioned at a favourable angle to make a H-bond interaction with the carbonyl group of enalaprilat.[16] The C-terminal part of the enalaprilat molecule has similar interactions as in the captopril complex. The N-terminal phenyl moiety at the P_1 position of enalaprilat is accommodated by hydrophobic interactions provided by Tyr496, Val502 and Val335, and these residues are conserved in tACE except for Tyr496, which is replaced with Phe512. A network of water molecules present at the S_2' subsite make indirect

interactions with the carboxy end of enalaprilat and additional residues in S_1' and S_2' (Asn261, Glu150 and Asp360) pockets similar to those in the captopril complex (Fig. 3b and Table 3).

Lisinopril

Lisinopril is a variant of enalapril with a long lysyl group at the P_1' position. In the inhibitor-bound structure, such as enalapril, the carboxy group of lisinopril coordinates tightly with the Zn^{2+} ion (coordinating distances are 1.89 and 2.57 Å). In addition, the inhibitor is bound to the protein through extensive H-bonds (16 in total, including 5 water-mediated H-bonds; Fig. 3c and Table 3). The orientation of the lisinopril molecule in AnCE is quite similar to that in the tACE–lisinopril complex.[15,16] The lysyl group at the P_1' position of lisinopril is held deep inside the S1′ pocket through ionic interactions with Glu150, Asp360 and Asp146. Similar ionic interactions of the lysyl group has been reported with Glu162 in the tACE–lisinopril structure.[15,16] The C-terminal carboxylate group of the inhibitor binds to residues Gln265, Lys495 and Tyr504 at the S_2' subsite. The amino group connecting the N-terminal phenyl and lysyl groups of lisinopril makes a strong H-bond with the backbone carbonyl oxygen of Ala338. In addition, a network of water molecules makes indirect interaction between the inhibitor and the residues at the S_1' and S_2' pockets of AnCE. One example of such an interaction involves the lysyl group of the inhibitor with residue Thr364 of AnCE. Even though the orientation of lisinopril is almost identical in both form I and form II structures, the orientation of the phenyl group at the P_1 position of lisinopril in form II is slightly different due to the presence of two Hepes molecules bound in the S_2 pocket.

Ramiprilat

Ramipril is a prodrug, an ethyl ester of ramiprilat, that is also a competitive inhibitor of ACE. It is derived from enalapril by extending a cyclopentane ring at the C-terminal proline moiety to a cyclopentane pyrrole ring. In the structure of the complex, an active form of ramipril, ramiprilat (as a result of hydrolysis in the crystallization medium), was observed. Like other carboxylate-based peptide inhibitors, ramiprilat also forms strong coordination with the Zn^{2+} ion (distances, 2.44 and 2.29 Å). In addition, some 12 H-bonds (including three water-mediated interactions) with the protein atoms were observed (Fig. 3d and Table 3). Similar to enalaprilat, ramiprilat also occupies S_1, S_1' and S_2' pockets of the protein at the active site. The cyclopentane ring at the C-terminal end of the inhibitor does not participate in any direct interaction with the protein; however, it has been reported that the bulky hydrophobic group at P_2' position has better potency for the C-domain of ACE, as in the case of trandolaprilat, a high-affinity ACE drug.[10]

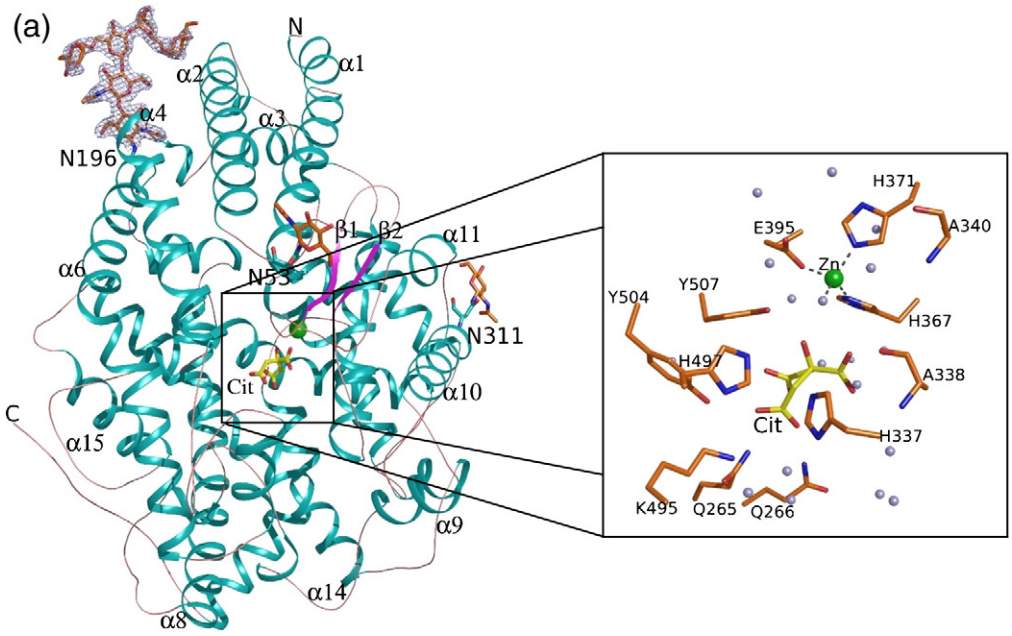

Fig. 2. (a) Overall topology of AnCE molecule. A cartoon representation shows an overview of native AnCE structure with active-site and N-glycosylated sugars (brown stick). The active-site residues (gold stick) and zinc ion (green sphere) are in the inset. Citrate ion at the active site is shown in stick model and labelled as Cit. Long-chain N-glycosylated sugars identified in all structures at Asn196 are shown in stick model calculated using an omit map contoured at 1σ. (b) Structure-based sequence comparison of AnCE with C-domain and N-domain of sACE. Helices and strands for AnCE are represented above the amino acid sequence with respective symbols. The secondary-structure elements are represented with the following codes: "A" for α-helices, "H" for 3_{10} helices and "S" for β-strands. Identical residues are colored in black and the zinc binding motif is shown in a box. The residues at different binding pockets, S_2, S_1, S_1' and S_2', are coloured yellow, green, magenta and cyan, respectively.

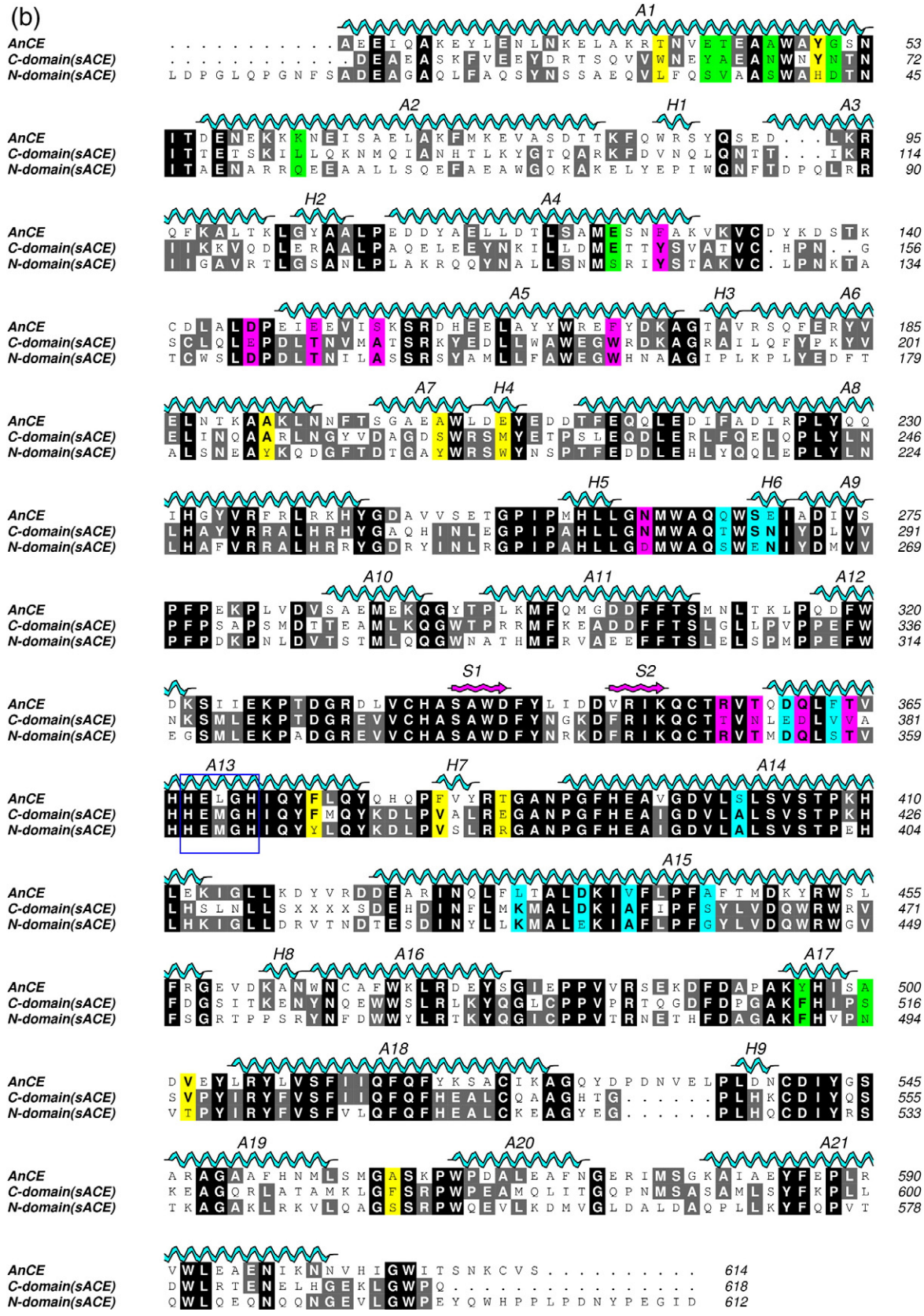

Fig. 2 (*legend on previous page*)

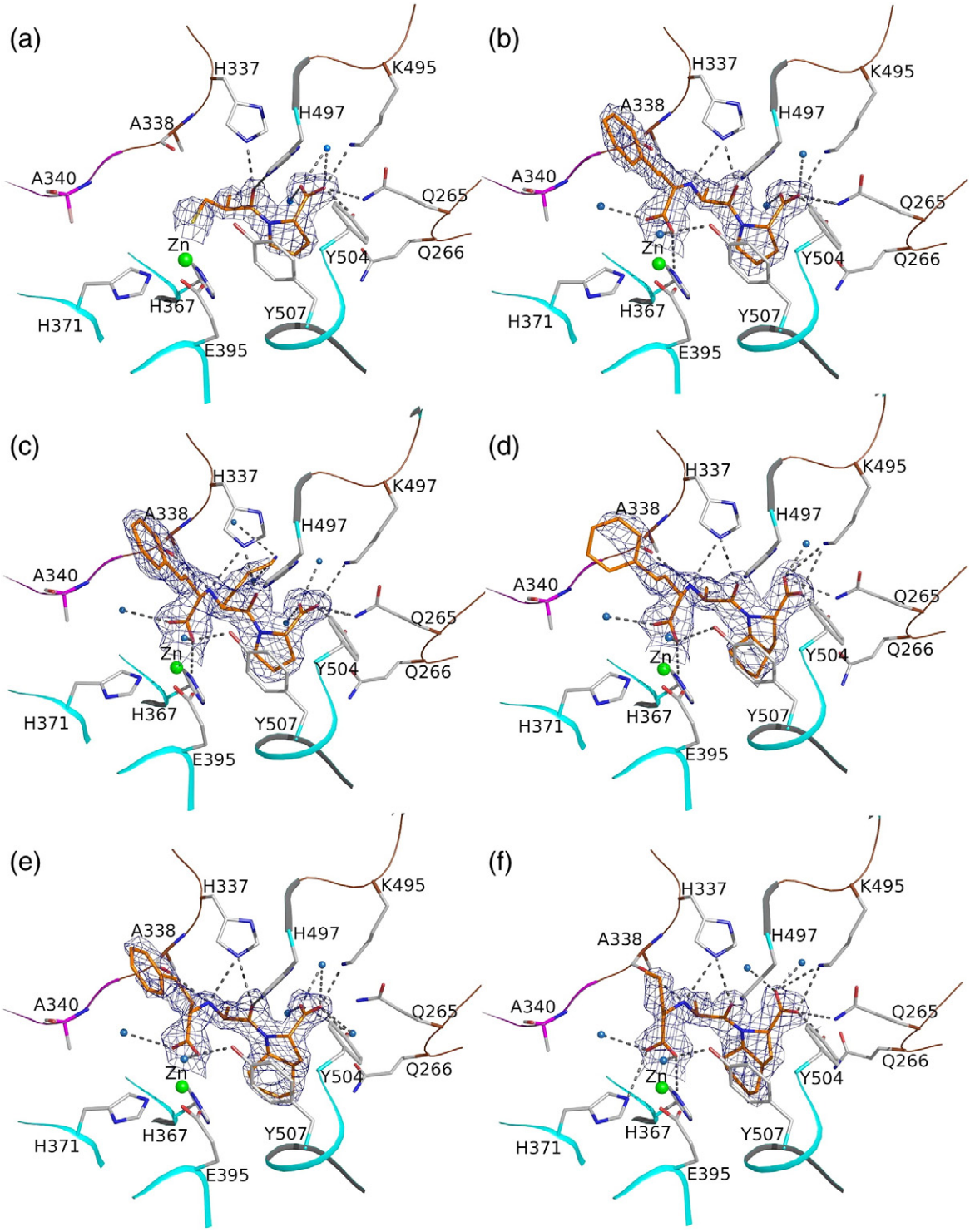

Fig. 3. Close-up of AnCE active site with bound antihypertensive drugs. The zinc ion is shown as a green sphere and water molecules in light blue. Atoms are coloured as follows: grey for carbon, red for oxygen, blue for nitrogen and purple for sulfur. Residues making H-bonds with the inhibitors are shown in stick representation. H-bonds are shown as dashed grey lines. Inhibitors are shown with omit map contoured at 1σ as light blue mesh: (a) Captopril, (b) enalaprilat, (c) lisinopril, (d) ramiprilat, (e) trandolaprilat and (f) perindoprilat.

Trandolaprilat

Trandolaprilat, an active form of trandolapril, is chemically similar to ramipril but has an octahydroindole ring in place of a cyclopentane pyrrole ring at the P_2' position of inhibitor, which occupies a slightly larger space at the S_2' pocket of the protein. The interactions of trandolaprilat with AnCE are identical to that of the AnCE–ramiprilat structure, including a strong Zn^{2+} ion coordination with the carboxylate group of the inhibitor (coordinating distances are 2.61 and 1.94 Å). The inhibitor binding is stabilized by 9 H-bond

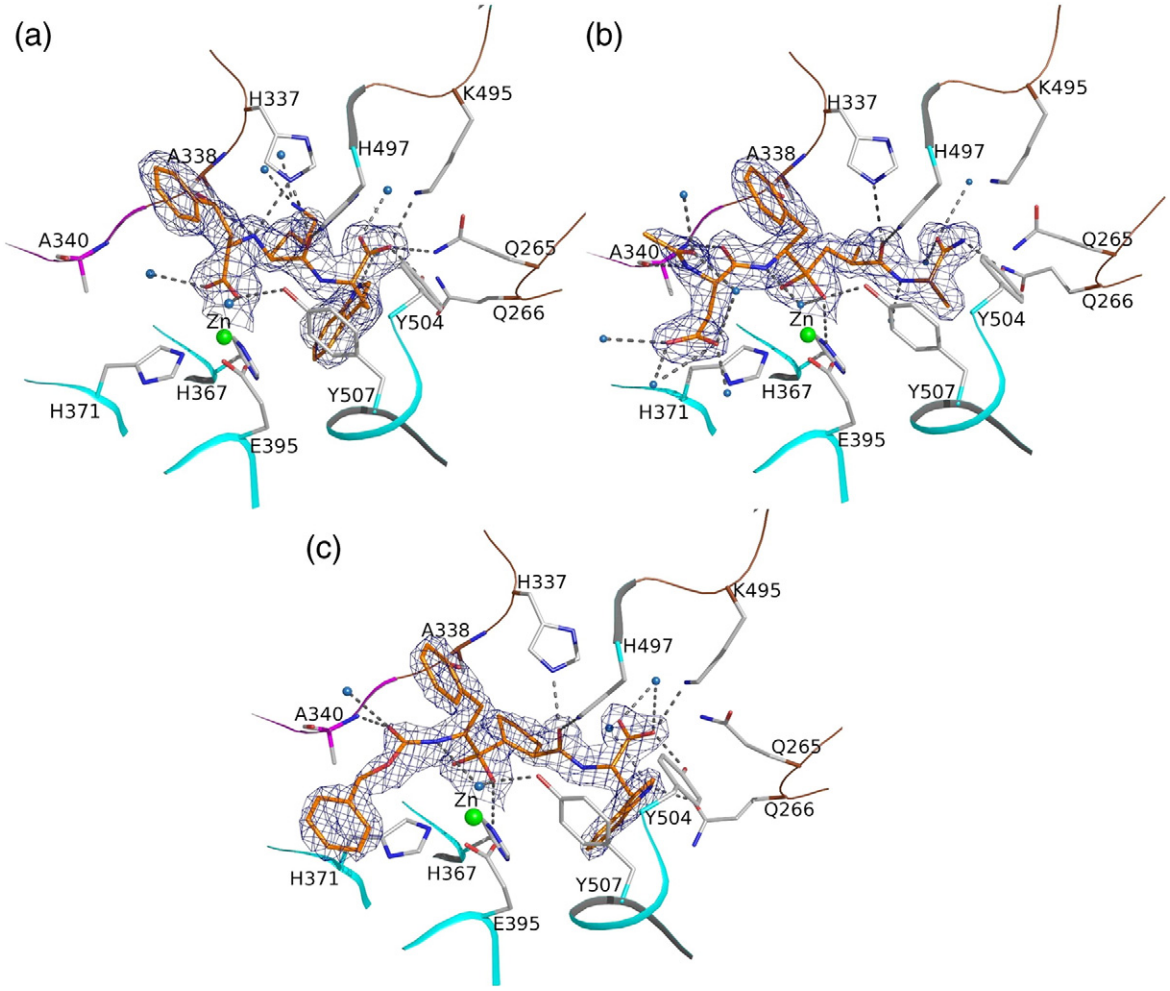

Fig. 4. Close-up of AnCE active site with new inhibitors bound. The representation and colour scheme are identical to those in Fig. 3. (a) LisW-S, (b) RXP407 and (c) RXPA380.

interactions with the protein and 5 H-bonds *via* water molecules (Fig. 3e and Table 3).

Perindoprilat

Perindoprilat, the active form, is chemically similar to trandolaprilat but has a propanoyl group instead of a phenyl group at the P_1 position of the inhibitor. In the structure of the complex, the inhibitor forms the expected strong coordination with the Zn^{2+} ion (distances, 1.91 and 2.59 Å) and 10 H-bonds with the protein atoms as well as four water-mediated interactions (Fig. 3f and Table 3). Compared to trandolaprilat, perindoprilat forms 3 additional H-bonds with Gln265, His367 and His371; however, the rest of the interactions are conserved in both structures of complexes.

Binding of newly designed inhibitors

Lisinopril–tryptophan derivative (lisW-S)

LisW-S is a lisinopril–tryptophan analogue inhibitor of ACE. It was derived from incorporating a tryptophan moiety in place of a proline moiety and has been shown to demonstrate selectivity toward the C-domain of the sACE.[31] In the AnCE complex, lisW-S binds tightly at the active site of the protein through 16 H-bonds, 10 with protein side chains and 6 with water molecules (Fig. 4a and Table 3). Similar to lisinopril, the lysyl group of lisW-S makes weak ionic interaction with Asp360 and Thr364 of AnCE. Compared to the lysyl chain in lisinopril, its orientation in lisW-S is slightly different and appears closer to Asp360 and Thr364. In addition, the lysyl group of the inhibitor makes indirect interactions with residues Asp146, Arg356 and Gln361 *via* a network of water molecules at the S_1' pocket of the protein. The phenyl moiety of the lisW-S is accommodated in a hydrophobic pocket, and the Zn^{2+} ion is coordinated by the carboxylate group of the inhibitor (distances, 1.82 and 2.84 Å) (Fig. 4a). Interestingly, the tryptophan moiety at the P_2' position of lisW-S appears to be oriented in a conformation different from that observed in RXPA380 in complex with AnCE (see below) and also different from the previously published tACE–RXPA380[17] and tACE–kAW (a keto-methylene derivative)[18] structures. In the present AnCE–lisW-S complex, the indole nitrogen atom of the tryptophan ring makes a new H-bond interaction with a conserved

Table 2. Comparison of substrate binding pockets in AnCE and sACE domains

	AnCE	C-domain	N-domain
S_2	T387	E403	R381
	F375	F391	Y369
	V502	V518	T496
	A560	F570	S548
	E207	M223	W201
	T40	W59	L32
	F383	V399	V377
	A203	S219	Y197
	Y50	Y69	H42
	A192	A208	Y186
S_1	A500	S516	N494
	Y496	F512	F490
	E124	E143	S119
	G51	N70	D43
	K62	L81	Q54
	E43	Y62	S35
	T44	A63	V36
	A47	N66	S39
S_1'	D146	E162	D140
	N261	N277	D255
	R356	T372	R350
	T358	N374	T352
	E150	T166	T144
	Q361	D377	Q355
	T364	V380	T358
	F169	W185	W163
	F127	Y146	Y122
	S154	A170	A148
S_2'	Q266	T282	S260
	F363	V379	S357
	S268	S284	E262
	D437	D453	E431
	V440	A456	A434
	A445	S461	G439
	S402	A418	A396
	L433	K449	K427
	D360	E376	D354
	E269	N285	N263

Asp399. Interestingly, it has been shown previously that Asp 399 in AnCE interacts indirectly with the catalytic Zn^{2+} ion, and mutation of this residue to Ala abrogates the activity of the protein.[32] In addition, the indole nitrogen atom makes a strong H-bond with the carbonyl oxygen of Glu395 (Glu411 in tACE), as well as with the side chains of Ser510, Lys438 and Asp437 *via* conserved water molecules at the S_2' pocket of the protein. It is worth noting that in ramiprilat, trandolaprilat and perindoprilat, the P_2' group is fused to the backbone of the molecule, whereas in lisW-S, two additional C–C bonds (Fig. 1) allow for more flexibility of the P_2' group functionality and further extension into the S_2' pocket. Thus, it appears that the orientation of the Trp moiety in the lisW-S inhibitor complex with AnCE adopts a more favourable conformation because of its potential interactions through the indole nitrogen atom of the ring.

RXPA380 phosphinic inhibitor (C-domain-selective inhibitor of sACE)

RXPA380 has been reported as the first highly selective inhibitor of the C-domain of sACE, able to differentiate between the two active sites of sACE by a selectivity factor of more than 3 orders of magnitude.[33] The RXPA380 molecule binds to AnCE in an extended conformation and occupies all four binding pockets, S_2, S_1, S_1' and S_2' (Fig. 4c and Table 3). The two phosphinyl oxygen atoms of the inhibitor make direct interaction with the catalytic Zn^{2+} ion (distances, 1.97 and 2.72 Å), as observed in the case of the tACE–RXPA380 complex.[17] These phosphinyl oxygen atoms are held together at opposite sides by H-bond interactions with Tyr507 and Glu368 (in addition to a weak H-bond interaction with His367; Table 3). This explains the asymmetric positioning of the PO_2 group above the Zn^{2+} ion. In addition, in the present AnCE-RXPA380 complex, the inhibitor is held by an additional H-bond provided by Gln266 with the Trp moiety of the RXPA380 at the P_2' position (Fig. 4c and Table 3). The Trp moiety of RXPA380 in the AnCE complex appears to have a slightly different orientation (tilted by some 10.8°) from that in the tACE–RXPA380 complex. This could be attributed to the large size of the S_2' subsite that allows for the accommodation of a bulky P_2' group in a number of different orientations. The orientation of the RXPA380 molecule in AnCE is favoured due to the H-bond interaction with the Gln266 (Thr282 in tACE). The RXPA380 molecule in AnCE is also held by 4 H-bonds mediated by water molecules (Table 3). Three of the four H-bonds are unique in the AnCE–RXPA380 structure. The amino-terminal phenyl moiety of the RXPA380 at the P_1 position is held by hydrophobic interactions provided by residues Tyr496, Val502, Trp341 and Val335. Another phenyl moiety at the P_2 position also appears to be accommodated by aromatic interaction with Phe375. This aromatic interaction is conserved in both AnCE and tACE in complex with RXPA380 and has been suggested to be a crucial residue for C-domain selectivity.[17,34] A network of water-molecule-mediated interactions is also observed at the S_1' pocket of the protein.

RXP407 phosphinic inhibitor (N-domain-selective inhibitor of sACE)

The RXP407 phosphinic peptide is a highly potent, selective and metabolically stable inhibitor of the N-domain of ACE (K_i=12 nM).[35] Like RXPA380, the interaction of the inhibitor RXP407 is also extensive and the inhibitor occupies all four binding subsites of the protein. Both the phosphinyl oxygen atoms directly coordinate with the catalytic Zn^{2+} ion (distances, 1.87 and 2.58 Å). In addition, the RXP407 molecule is anchored by 7 H-bonds between the inhibitor and protein atoms and 12 H-bonds between the inhibitor and water molecules (Fig. 4b and Table 3). The carboxy terminus of the inhibitor is held by a network of H-bonds mediated by water molecules and an indirect interaction with Asn261. In addition, the C-terminal amide nitrogen and carbonyl oxygen are involved in weak ionic interactions with Gln265. With the exception of a few, all other observed H-bonds in the AnCE–RXPA380

Table 3. Comparison of H-bond interactions at the active site of AnCE due to inhibitor binding

Captopril			Enalaprilat			Lisinopril			Ramiprilat			Trandolaprilat		
Ligand atoms	Interacting atoms	Distance (Å)	Ligand atoms	Interacting atoms	Distance (Å)	Ligand atoms	Interacting atoms	Distance (Å)	Ligand atoms	Interacting atoms	Distance (Å)	Ligand atoms	Interacting atoms	Distance (Å)
O2	Q265NE2	3.13	O5	Q265NE2	3.27	O5	Q265NE2	3.23	OAC	Q265NE2	3.28	N	H337NE2	3.01
O1	H337NE2	2.65	O4	Q265NE2	3.21	O4	Q265NE2	3.17	O	H337NE2	2.78	O	H337NE2	2.85
O2	K495NZ	2.72	O1	H337NE2	2.71	O1	H337NE2	2.73	N	H337NE2	3.10	N	A338O	2.95
O1	H497NE2	2.92	N1	H337NE2	3.02	N1	H337NE2	3.06	N	A338O	3.01	OAC	K495NZ	2.61
O2	Y504OH	2.6	N1	A338O	3.09	N1	A338O	2.94	OAT	H367NE2	3.30	O	H497NE2	2.86
O3	Wat	2.67	O2	H367NE2	3.42	O3	H367NE2	3.33	OAC	K495NZ	3.34	OAC	Y504OH	2.48
O3	Wat	2.80	O4	K495NZ	2.75	N1	E368OE3	3.45	OAF	K495NZ	3.01	OAB	Y507OH	2.66
O2	Wat	3.37	O4	Y504OH	2.56	O4	K495NZ	2.82	OAF	Y504OH	2.33	OAE	Wat	2.36
			O2	Y507OH	2.74	O4	Y504OH	2.58	OAT	Y507OH	2.88	OAB	Wat	3.38
			O5	Wat	2.60	O3	Y507OH	2.73	OAC	Wat	2.46	OAF	Wat	2.65
			O5	Wat	2.54	O5	Wat	2.73	OAT	Wat	3.26	OAF	Wat	3.27
			O4	Wat	3.38	O5	Wat	2.68	OAD	Wat	2.84	OAF	Wat	2.67
			O3	Wat	2.76	N3	Wat	3.49				OAC	Wat	3.45
			O2	Wat	3.28	N3	Wat	3.13				OAC	Wat	2.98
						O3	Wat	3.21						
						O2	Wat	2.86						

Perindoprilat			lisW-S			RXPA380			RXP407		
Ligand atoms	Interacting atoms	Distance (Å)	Ligand atoms	Interacting atoms	Distance (Å)	Ligand atoms	Interacting atoms	Distance (Å)	Ligand atoms	Interacting atoms	Distance (Å)
OAG	Q265NE2	3.08	OAC	Q265NE2	3.09	N3	Q266OE1	3.09	OAH	H337NE2	2.86
O	H337NE2	2.79	OAD	H337NE2	2.72	O5	H337NE2	2.75	OAI	A340N	2.95
N	H337NE2	3.06	N	H337NE2	2.97	O2	A340N	2.57	NAU	A340O	2.78
N	A338O	3.01	N	A338O	2.99	O3	H367NE2	3.38	OAJ	H367NE2	3.21
OAE	H367NE2	3.41	OAC	K495NZ	2.69	O6	K495NZ	2.67	OAH	H497NE2	2.97
OAQ	H371NE2	2.93	OAD	H497NE2	2.87	O5	H497NE2	2.80	NAD	Y504OH	2.58
OAD	K495NZ	3.21	OAC	Y504OH	2.47	O6	Y504OH	2.54	OAJ	Y507OH	2.86
OAG	K495NZ	2.81	O	Y507OH	2.8	O3	Y507OH	2.69	NAW	Wat	2.87
OAG	Y504OH	2.36	NAZ	Wat	2.93	O4	E368OE1	2.48	OAK	Wat	2.73
OAE	Y507OH	2.64	OAF	Wat	2.65	O2	Wat	3.00	OAK	Wat	3.32
OAD	Wat	2.44	NAA	Wat	2.62	N1	Wat	3.32	OAK	Wat	3.26
OAD	Wat	3.38	NAA	Wat	2.60	O3	Wat	3.26	OAG	Wat	2.70
OAE	Wat	3.33	OXT	Wat	2.87	O6	Wat	3.39	OAG	Wat	2.98
OAQ	Wat	2.90	O	Wat	3.34	OXT	Wat	2.87	OAE	Wat	2.91
						OXT	Wat	2.65	OAE	Wat	2.96
						N3	Wat	3.43	N	Wat	2.83
									O	Wat	3.08
									O	Wat	2.99

complex are also present in the AnCE–RXP407 complex. The N-terminal carbonyl oxygen forms a network of water-mediated interactions and also participates in an indirect interaction with Arg506. In addition, the aspartic side chain at the P_2 position of the inhibitor interacts indirectly with His394 and Tyr378 *via* water molecules. Unlike the RXPA380 inhibitor, the RXP407 molecule does not participate in hydrophobic interactions due to lack of bulky groups at the P_2 and P_2' positions.

Based on the present AnCE–RXP407 complex, the RXP407 inhibitor site was docked in the active site of the N-domain of sACE and the potential interactions were analysed. Apart from direct interaction of phosphinyl oxygen atoms with the catalytic Zn^{2+} ion (Fig. 5), the RXP407 molecule appears to be held in the active site through 9 H-bonds with the protein atoms. Interestingly, the aspartic acid group of the RXP407 molecule forms an H-bond with Tyr369 in the N-domain protein, which is in fact replaced by Phe in both AnCE (Phe375) and tACE (Phe381). This has been reported as a crucial residue for the selectivity of the phosphinic inhibitor toward the N- and C-domains in sACE.[35] In addition, the aspartic acid of RXP407 in the N-domain also seems to mediate weak ionic interaction with Arg381, and this residue is replaced with Thr387 and Glu403 in AnCE and tACE, respectively. Thus, these two important residues at the S_2 subsite of the N-domain contribute to the selectivity of the RXP407 over the RXPA380. Other direct interactions appear to be conserved in the modelled N-domain sACE–RXP407 structure.

Conserved active-site water structure

A comparison of the active site of all 10 structures reported here shows that apart from displacing few water molecules from the active site, the rest of the water molecules are conserved following the binding of inhibitors (Table 3). Among the two water molecules in the captopril (smallest inhibitor studied) complex that interact with the inhibitor, one is conserved in the native structure. Amongst other inhibitors with the Phe moiety at P_1 and the lysyl moiety of P_1' positions are observed to displace one conserved water molecule from each site. Few other water molecules that interact with the inhibitors are conserved in almost all structures of complexes. The perindoprilat complex shows four water molecules interacting with the inhibitor at the active site; all but one are conserved in other structures. The additional groups attached at the N-terminal end of RXPA380 and RXP407 phosphinic inhibitors at the P_2 position displace two and four conserved water molecules from the S_2 subsite, respectively. The Trp moiety of lisW-S and RXPA380 at the S_2' subsite also displace four and three water molecules, respectively. The cluster of water molecules that form a network of H-bonds with these inhibitors are conserved except one water molecule from each lisW-S, RXPA380 and three water molecules from RXP407 complexes. Moreover, a network of water molecules at the S_1' subsite, which make H-bond interactions with the side chain of Asn261, Glu150, Arg356, Gln361, Thr364, and Asp360, is conserved in all structures of complexes. In addition, a cluster of water molecules at the S_2' subsite that interacts with Asp399, Lys438, Gln266 and Gln265 is also conserved in all structures.

Structural implications on inhibitor potencies

It has been shown previously that captopril is a highly potent inhibitor for AnCE,[24] C- and N-domains of sACE with K_i values of 11, 14 and 8.9 nM, respectively.[10] Thus, the binding potency of captopril for AnCE is somewhat similar, as in the case of tACE and for the N-domain of ACE at 300 mM NaCl concentration. On the other hand, enalaprilat is a better inhibitor for the C-domain, and binding affinity has been reported to be 40- and 4-fold higher (at 300 mM NaCl concentration) compared to the AnCE[24] and N-domain, res-

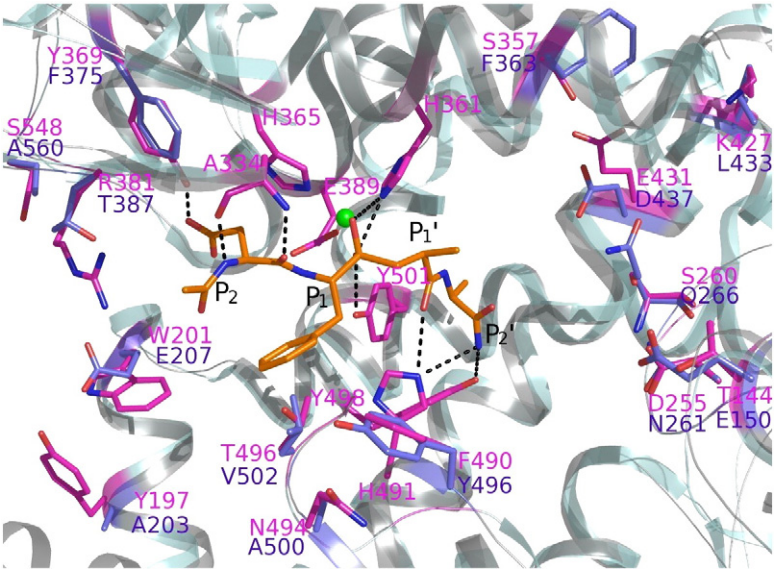

Fig. 5. Potential binding mode of RXP407 (shown in stick representation) with the N-domain of sACE. The modelling was based on superposition of active-site residues from AnCE (AnCE–RXP407 complex) onto the N-domain of sACE. Possible H-bonds are shown in black dashed lines. Conserved residues in AnCE and N-domain are shown as pink sticks. Other structurally equivalent residues are labelled in pink and blue for N-domain and AnCE, respectively.

pectively.[10] The hydrophobic S_1 pocket of tACE has been suggested as a crucial determinant for enalaprilat binding;[16] however, replacement of Phe512 with Tyr496 in AnCE probably makes this pocket less hydrophobic. Lisinopril is a highly efficient inhibitor of the C-domain of sACE and binds with a K_i of 2.4 nM, but has been shown to have lower affinity for AnCE (K_i of 180 nM)[24] and the N-domain (K_i of 44 nM).[10] The ionic interactions of the lysyl group at the P_1' position with the charged residues Glu162 and Glu376 at the S_1' subsite of the C-domain might contribute to the enhanced specificity. These ionic interactions are lost due to replacement of the corresponding residues with a shorter charged residue, Asp in both AnCE and the N-domain protein of sACE. Trandolapril and perindopril are high-affinity ACE drugs, whose potency for AnCE has been reported to be 3 orders of magnitude lower than that for the C-domain[24] and 2 orders lower than that for the N-domain.[10] Similarly, the low affinity of AnCE for trandolaprilat and perindoprilat is probably because of a less hydrophobic S_1 pocket. Furthermore, the binding potency of lisW-S with AnCE was investigated. Despite some of the potential interactions of the Trp moiety of lisW-S with the residues at the S_2' pocket, the observed potency is almost 60-fold lower than that of its parent compound lisinopril ($K_i = 11.3\ \mu M$). However, this K_i value for AnCE is comparable with the previously determined K_i value of lisW-S for the C-domain (7 μM), which is more than 100-fold selective than for the N-domain of sACE.[31] The better selectivity for the C-domain as well as AnCE over the N-domain may be attributed largely to P_2' orientation and its interactions with residues in the S_2' pocket.

RXPA380 is a domain-selective inhibitor, which has a K_i of 3 nM for the C-domain, 3000 times lower than that for the N-domain.[33] It has been demonstrated previously that bulky hydrophobic residue at the P_2' position makes RXPA380 and kAW high-affinity inhibitors for the C-domain.[18] The potency of RXPA380 for AnCE was investigated ($K_i = 94\ \mu M$) and found to be almost 30,000 fold lower than that of C-domain.[26] However, based on our new structural data, we have demonstrated that RXPA380 is able to bind efficiently to AnCE. A possible explanation (based on the structure) for the low affinity in AnCE may be due to changes in residues at the binding pockets. For example, at the S_1 pocket, Phe512 and Val518 in tACE, which provide a hydrophobic pocket for the RXPA380 affinity, are replaced by Tyr496 and Val502 in AnCE. Secondly, the Trp moiety of the RXPA380 in tACE is almost equidistant from Val379 and Val380, which form the lining of the S_2' subsite, and these residues are replaced by Phe363 and Thr364 in AnCE. Although RXPA380 makes similar interactions in both tACE and AnCE, the hydrophobic interactions that contribute to the inhibitor binding at different subsites seem to have differences in the two proteins that might also have a crucial impact on the affinity and potency of the inhibitor.

The K_i value of RXP407 for AnCE has been reported as 2200 nM,[25] approximately 180-fold higher than that for the N-domain, which has a K_i value of 12 nM).[35] The difference in potency of the RXP407 inhibitor for these proteins is likely due to the fact that the N-domain displays nine interactions, two more than that of the AnCE for RXP407, as evident from the structural data. Apart from these interactions, interestingly, the aspartic group of the RXP407 is likely to make ionic interaction with Arg381 in the N-domain and this interaction is lost in AnCE due to the presence of Thr387 at the equivalent position. In support of this, it has been reported recently that a double mutant containing the Tyr369-to-Phe change as well as Arg381-to-Glu displayed a 100-fold decrease in binding affinity, confirming that the S_2 pocket plays a major role in RXP407 selectivity in the N-domain protein.[34] In addition, the single Arg381-to-Glu mutation only caused a 6-fold difference in the K_i of the N-domain for RXP407 and the Tyr369-to-Phe mutation had little effect on binding to this inhibitor.[34]

Conclusions

The structural data presented in this report on AnCE in complex with nine inhibitors show how these potent inhibitors occupy different binding pockets at the active site of the protein. Although there are subtle differences in binding, this ACE homologue has preserved function and several active-site interactions are conserved, which highlights the general structural conservation. The structures of AnCE in complex with RXPA380 and lisW-S show different orientations of the Trp moiety at the P_2' site, which might be largely responsible for the domain selectivity, emphasising the large size of the S_2' pocket. This suggests that a careful exploitation of the large S_2' subsite and interaction of a bulkier side chain with specific residues in the S_2' pocket might provide a lead to achieve further domain selectivity. Similarly, the structure of RXP407 with AnCE has provided the first glimpse of how this inhibitor would bind at the active site and the details of a different set of interactions that could be modelled onto the N-domain structure of sACE in order to understand the enhanced specificity. In addition, the conserved water molecules at both S_1' and S_2' of the active site could be exploited to extend the inhibitor length or for insertion of new chemical groups that might favour interactions with charged side-chain residues at these subsites. This knowledge will now provide a basic structural framework for further improvement of domain-specific inhibitors of sACE.

Materials and Methods

Protein expression and purification

AnCE was cloned and expressed in *Pichia pastoris* as described previously.[36] In brief, AnCE was purified to homogeneity from culture media using hydrophobic

interaction chromatography and size-exclusion chromatography. The induced culture media was treated with ammonium sulfate to a final concentration of 1.5 M containing 20 mM Tris (pH 8.0). After centrifugation and filtration, the culture supernatant was loaded onto a phenyl-Sepharose Fast Flow 6 column, which was preequilibrated with 20 mM Tris (pH 8.0) and 1.5 M ammonium sulfate. The bound protein was eluted with a decreasing gradient of ammonium sulfate (1.5–0 M). The protein-containing fractions were pooled and concentrated and applied to a Superdex 200 size-exclusion column preequilibrated with 20 mM Tris (pH 8.0) and 150 mM NaCl. A single homogeneous peak of protein was collected, dialysed [5 mM Hepes (pH 7.5) and 0.1 mM PMSF] and finally concentrated to ~26 mg/ml and stored at −80 °C.

Antihypertensive drugs and new inhibitors

Synthesis of RXPA380,[33] RXP407, Ac-Asp-$_{(L)}$Phe(PO_2CH_2)$_{(L)}$Ala-Ala-NH_2[35] and lisW-S[31] were described previously. All six antihypertensive drugs were purchased from Sigma-Aldrich. Detailed chemical structure of all the inhibitors are shown in Fig. 1.

X-ray crystallography

A total of 400 different crystallization conditions were screened with the help of a Phoenix protein crystallization robot (Art Robbins Instruments) in sitting-drop vapour-diffusion method at 16 °C. After optimisation, crystals for native AnCE were obtained with 2 μl of the native AnCE [10 mg/ml in 5 mM Hepes (pH 7.5), 0.1 mM PMSF and 10 μM zinc acetate] mixed with an equal volume of reservoir solution [100 mM Hepes (pH 7.5) and 1.3 M sodium citrate] and suspended above the well as a hanging drop. The crystals of AnCE in complex with the antihypertensive drugs (captopril, enalaprilat, lisinopril, ramiprilat, trandolaprilat, perindoprilat), the lisinopril derivative lisW-S and domain-selective phosphinic peptidyl inhibitors RXPA380 and RXP407 were obtained by co-crystallization. Briefly, native AnCE was preincubated with the inhibitors (protein/inhibitor molar ratio of 1:6) on ice for 5 h before crystallization under native AnCE crystallization condition. Diffraction-quality crystals of both native AnCE and the inhibitor complexes appeared after 1 week. All X-ray diffraction data up to 1.85 Å were collected (for both native AnCE and the inhibitor complexes) at Diamond Light Source (Oxon, UK) on stations IO2, IO3 and IO4. No cryoprotectant was used to keep the crystal at constant temperature under the liquid nitrogen jet during data collection. For each data set, 100 images were collected by using a Quantum-4 charge-coupled device detector (ADSC Systems, CA). Raw data images were indexed and scaled with HKL2000 software package.[37] All crystals belonged to primitive rhombohedral *R*3 space group with one molecule of AnCE per asymmetric unit. Data reduction was carried out with the CCP4 program TRUNCATE[38] (Table 1).

Initial phases for structure solution were obtained with the molecular replacement routines of PHASER program.[39] Native AnCE [Protein Data Bank (PDB) code 1J38, form I in monoclinic space group $P2_1$ at 2.6 Å resolution][27] was used as the search model. The resultant model was refined using REFMAC5.[40] Five percent of reflections were separated as the R_{free} set and used for cross-validation.[41] After an initial round of rigid-body refinement, rounds of restrained refinement with electron density map calculations and manual adjustments of the model using COOT[28] were carried out. On the basis of F_o-F_c electron density, side-chain atoms were omitted at some positions. Water molecules were added at positions where F_o-F_c electron density peaks exceeded 3σ and potential H-bonds could be made. Detailed refinement statistics for all the structures are given in Table 1. A similar approach was adopted to solve all nine inhibitor-bound structures of complexes using the refined native AnCE structure as the starting model. Based on electron density interpretation, ligands were added in their respective structure and further refinement was carried out. The coordinate and parameter files for the drug molecules/inhibitors were generated using the PRODRG server.[42] Validation was conducted with the aid of programs PROCHECK[43] and MOLPROBITY.[44] There were no residues in the disallowed region of the Ramachandran plot. Figures were drawn with PyMOL (DeLano Scientific, San Carlos, CA). H-bonds were verified with the program HBPLUS.[45]

PDB accession codes

The atomic coordinates and structure factors for all 10 structures [codes 2x8y (native), 2x8z (captopril complex), 2x90 (enalaprilat complex), 2x91 (lisinopril complex), 2x92 (ramiprilat complex), 2x93 (trandolaprilat complex), 2x94 (perindoprilat complex), 2x95 (isinopril-tryptophan analogue, lisW-S complex), 2x96 (RXPA380 complex) and 2x97 (RXP407 complex)] have been deposited in the PDB.

Acknowledgements

This work was supported by the Medical Research Council (UK) through a project grant (81272) and a Royal Society (UK) Industry Fellowship to K.R.A. We thank the scientists at stations IO2, IO3 and IO4 of Diamond Light Source (Didcot, Oxon, UK) and Nethaji Thiyagarajan for their support during X-ray diffraction data collection. We also thank Pierre Corvol and Tracy Williams of INSERM, College de France (Paris, France), for providing *P. pastoris* expressing AnCE.

References

1. Acharya, K. R., Sturrock, E. D., Riordan, J. F. & Ehlers, M. R. W. (2003). ACE revisited: a new target for structure-based drug design. *Nat. Rev. Drug Discov.* **2**, 891–902.
2. Turner, A. T. & Hooper, N. M. (2002). The angiotensin-converting enzyme gene family: genomics and pharmacology. *Trends Pharmacol. Sci.* **23**, 177–183.
3. Eriksson, U., Danilczyk, U. & Penninger, J. M. (2002). Just the beginning: novel functions for angiotensin-converting enzymes. *Curr. Biol.* **12**, 745–752.
4. Ehlers, M. R. W. & Riordan, J. F. (1989). Angiotensin-converting enzyme: new concepts concerning its biological role. *Biochemistry*, **28**, 5311–5318.
5. Unger, T. (2002). The role of the renin–angiotensin system in the development of cardiovascular disease. *Am. J. Cardiol.* **89**, 3A–9A.

6. Soubrier, F., Alhenc-Gelas, F., Hubert, C., Allegrini, J., John, M., Tregear, G. & Corvol, P. (1988). Two putative active centers in human angiotensin I-converting enzyme revealed by molecular cloning. *Proc. Natl Acad. Sci. USA*, **85**, 9386–9390.
7. Ehlers, M. R. W., Fox, E. A., Strydom, D. J. & Riordan, J. F. (1989). Molecular cloning of human testicular angiotensin-converting enzyme: the testis isozyme is identical to the C-terminal half of endothelial angiotensin-converting enzyme. *Proc. Natl Acad. Sci. USA*, **86**, 7741–7745.
8. Voronov, S., Zueva, N., Orlov, V., Arutyunyan, A. & Kost, O. (2002). Temperature-induced selective death of the C-domain within angiotensin-converting enzyme molecule. *FEBS Lett.* **522**, 77–82.
9. Sturrock, E. D., Yu, X. C., Wu, Z., Biemann, K. & Riordan, J. F. (1996). Assignment of free and disulfide-bonded cysteine residues in testis angiotensin-converting enzyme: functional implications. *Biochemistry*, **35**, 9560–9566.
10. Wei, L., Clauser, E., Alhenc-Gelas, F. & Corvol, P. (1992). The two homologous domains of human angiotensin I-converting enzyme interact differently with competitive inhibitors. *J. Biol. Chem.* **267**, 13398–13405.
11. Jaspard, E., Wei, L. & Alhenc-Gelas, F. (1993). Differences in the properties and enzymatic specificities of the two active sites of angiotensin I-converting enzyme (kininase II). Studies with bradykinin and other natural peptides. *J. Biol. Chem.* **268**, 9496–9503.
12. Rousseau, A., Michaud, A., Chauvet, M. T., Lenfant, M. & Corvol, P. (1995). The hemoregulatory peptide *N*-acetyl-Ser-Asp-Lys-Pro is a natural and specific substrate of the N-terminal active site of human angiotensin-converting enzyme. *J. Biol. Chem.* **270**, 3656–3661.
13. Deddish, P. A., Marcic, B., Jackman, H. L., Wang, H. Z., Skidgel, R. A. & Erdös, E. G. (1998). N-domain–specific substrate and C-domain inhibitors of angiotensin-converting enzyme: angiotensin-(1–7) and keto-ACE. *Hypertension*, **31**, 912–917.
14. Deddish, P. A., Jackman, H. L., Skidgel, R. A. & Erdös, E. G. (1997). Differences in the hydrolysis of enkephalin congeners by the two domains of angiotensin converting enzyme. *Biochem. Pharmacol.* **53**, 1459–1463.
15. Natesh, R., Schwager, S. L. U., Sturrock, E. D. & Acharya, K. R. (2003). Crystal structure of the human angiotensin-converting enzyme-lisinopril complex. *Nature*, **421**, 551–554.
16. Natesh, R., Schwager, S. L. U., Evans, H. R., Sturrock, E. D. & Acharya, K. R. (2004). Structural details on the binding of antihypertensive drugs captopril and enalaprilat to human testicular angiotensin I-converting enzyme. *Biochemistry*, **43**, 8718–8724.
17. Corradi, H. R., Chitapi, I., Sewell, B. T., Georgiadis, D., Dive, V., Sturrock, E. D. & Acharya, K. R. (2007). The structure of testis angiotensin-converting enzyme in complex with the C domain-specific inhibitor RXPA380. *Biochemistry*, **46**, 5473–5478.
18. Watermeyer, J. M., Kröger, W. L., O'Neill, H. G., Sewell, T. & Sturrock, E. D. (2008). Probing the basis of domain-dependent inhibition using novel ketone inhibitors of angiotensin-converting enzyme. *Biochemistry*, **47**, 5942–5950.
19. Watermeyer, J. M., Kröger, W. L., O'Neill, H. G., Sewell, T. & Sturrock, E. D. (2010). Characterization of domain selective inhibitor binding in angiotensin-converting enzyme using a novel derivative of lisinopril. *Biochem. J.* **428**, 67–74.
20. Corradi, H. R., Schwager, S. L. U., Nchinda, A. T., Sturrock, E. D. & Acharya, K. R. (2006). Crystal structure of the N domain of human somatic angiotensin I-converting enzyme provides a structural basis for domain-specific inhibitor design. *J. Mol. Biol.* **357**, 964–974.
21. Cushman, D. W., Cheung, H. S., Sabo, E. F. & Ondetti, M. A. (1977). Design of potent competitive inhibitors of angiotensin-converting enzyme. Carboxyalkanoyl and mercaptoalkanoyl amino acids. *Biochemistry*, **16**, 5484–5491.
22. Steckelings, U. M, Artuc, M., Wollschläger, T., Wiehstutz, S. & Henz, B. M. (2001). Angiotensin-converting enzyme inhibitors as inducers of adverse cutaneous reactions. *Acta Derm.-Venereol.* **81**, 321–325.
23. Cornell, M. J., Williams, T. A., Lamango, N. S., Coates, D., Corvol, P., Soubrier, F. *et al.* (1995). Cloning and expression of an evolutionary conserved single-domain angiotensin converting enzyme from *Drosophila melanogaster*. *J. Biol. Chem.* **270**, 13613–13619.
24. Williams, T. A., Michaud, A., Houard, X., Chauvet, M. T., Soubrier, F. & Corvol, P. (1996). *Drosophila melanogaster* angiotensin I-converting enzyme expressed in *Pichia pastoris* resembles the C domain of the mammalian homologue and does not require glycosylation for secretion and enzymic activity. *Biochem. J.* **318**, 125–131.
25. Coates, D., Isaac, R. E., Cotton, J., Siviter, R., Williams, T. A., Shirras, A. & Dive, V. (2000). Functional conservation of the active sites of human and *Drosophila* angiotensin I-converting enzyme. *Biochemistry*, **39**, 8963–8969.
26. Bingham, R. J., Dive, V., Phillips, S. E. V., Shirras, A. D. & Isaac, R. E. (2006). Structural diversity of angiotensin-converting enzyme. *FEBS J.* **273**, 362–373.
27. Kim, H. M., Shin, D. R., Yoo, O. J., Lee, H. & Lee, J. O. (2003). Crystal structure of *Drosophila* angiotensin I-converting enzyme bound to captopril and lisinopril. *FEBS Lett.* **538**, 65–70.
28. Emsley, P. & Cowtan, K. (2004). Coot: Model building tools for molecular graphics. *Acta Crystallogr., Sect. D: Biol. Crystallogr.* **60**, *2126–2132.*
29. Gordon, K., Redelinghuys, P., Schwager, S. L. U., Ehlers, M. R. W., Papageorgiou, A. C., Natesh, R. & Acharya, K. R. (2003). Deglycosylation, processing and crystallization of human testis angiotensin-converting enzyme. *Biochem. J.* **371**, 437–442.
30. Schechter, I. & Berger, A. (1967). On the size of the active site in proteases. *Biochem. Biophys. Res. Commun.* **27**, 157–162.
31. Nchinda, A. T., Chibale, K., Redelinghuys, P. & Sturrock, E. D. (2006). Synthesis and molecular modeling of a lisinopril-tryptophan analogue inhibitor of angiotensin I-converting enzyme. *Bioorg. Med. Chem. Lett.* **16**, 4616–4619.
32. Williams, T. A., Corvol, P. & Soubrier, F. (1994). Identification of two active site residues in human angiotensin I-converting enzyme. *J. Biol. Chem.* **269**, 29430–29434.
33. Georgiadis, D., Cuniasse, P., Cotton, J., Yiotakis, A. & Dive, V. (2004). Structural determinants of RXPA380, a potent and highly selective inhibitor of the angiotensin-converting enzyme C-domain. *Biochemistry*, **43**, 8048–8054.
34. Kröger, W. L., Douglas, R. G., O'Neill, H. G., Dive, V. & Sturrock, E. D. (2009). Investigating the domain

specificity of phosphinic inhibitors RXPA380 and RXP407 in angiotensin-converting enzyme. *Biochemistry*, **48**, 8405–8412.
35. Dive, V., Cotton, J., Yiotakis, A., Michaud, A., Vassiliou, S., Jiracek, J. *et al.* (1999). RXP 407, a phosphinic peptide, is a potent inhibitor of angiotensin I converting enzyme able to differentiate between its two active sites. *Proc. Natl Acad. Sci. USA*, **96**, 4330–4335.
36. Houard, X., Williams, T. A., Michaud, A., Dani, P., Isaac, R. E., Shirras, A. D. *et al.* (1998). The *Drosophila melanogaster*-related angiotensin-I-converting enzymes Acer and Ance—distinct enzymic characteristics and alternative expression during pupal development. *Eur. J. Biochem.* **257**, 599–606.
37. Otwinowski, Z. & Minor, W. (1997). Processing of X-ray diffraction data collected in oscillation mode. *Methods Enzymol.* **276**, 307–326.
38. Collaborative Computational Project Number 4 (1994). The CCP4 suite: Programs for protein crystallography. *Acta Crystallogr., Sect. D: Biol. Crystallogr.* **50**, *760–763.*
39. McCoy, A. J., Grosse-Kunstleve, R. W., Adams, P. D., Winn, M. D., Storoni, L. C. & Read, R. J. (2007). PHASER crystallographic software. *J. Appl. Crystallogr.* **40**, 658–674.
40. Murshudov, G. N. (1997). Refinement of macromolecular structures by the maximum-likelihood method. *Acta Crystallogr., Sect. D: Biol. Crystallogr.* **53**, *240–255.*
41. Brünger, A. T. (1992). Free *R* value: a novel statistical quantity for assessing the accuracy of crystal structures. *Nature*, **355**, 472–475.
42. Schuettelkopf, A. W. & van Aalten, D. M. F. (2004). PRODRG: a tool for high-throughput crystallography of protein-ligand complexes. *Acta Crystallogr., Sect. D: Biol. Crystallogr.* **60**, *1355–1363.*
43. Laskowski, R. A., MacArthur, M. W., Moss, D. S. & Thornton, J. M. (1993). PROCHECK—a program to check the stereo-chemical quality of protein structures. *J. Appl. Crystallogr.* **26**, 283–291.
44. Davis, I. W., Murray, L. W., Richardson, J. S. & Richardson, D. C. (2004). MOLPROBITY: structure validation and all-atom contact analysis for nucleic acids and their complexes. *Nucleic Acids Res.* **32**, 615–619.
45. McDonald, I. K. & Thornton, J. M. (1994). Satisfying hydrogen bonding potential in proteins. *J. Mol. Biol.* **238**, 777–793.